Uptake and Subcellular Distribution of [^{3}H]Arachidonic Acid in Murine Fibrosarcoma Cells Measured by Electron Microscope Autoradiography

ELLIS J. NEUFELD,* PHILIP W. MAJERUS,* CHARLES M. KRUEGER,‡ and JEFFREY E. SAFFITZ‡

Division of Hematology-Oncology, Departments of Internal Medicine and Biological Chemistry, and ‡Department of Pathology and Cardiovascular Division, Washington University School of Medicine, St. Louis, Missouri 63110. Reprint requests should be addressed to J. E. Saffitz.

ABSTRACT We have used quantitative electron microscope autoradiography to study uptake and distribution of arachidonate in $HSDM_1C_1$ murine fibrosarcoma cells and in EPU-1B, a mutant $HSDM_1C_1$ line defective in high affinity arachidonate uptake. Cells were labeled with [^{3}H]arachidonate for 15 min, 40 min, 2 h, or 24 h. Label was found almost exclusively in cellular phospholipids; 92–96% of incorporated radioactivity was retained in cells during fixation and tissue processing. All incorporated radioactivity was found to be associated with cellular membranes. Endoplasmic reticulum (ER) contained the bulk of [^{3}H]arachidonate at all time points in both cell types, while mitochondria, which contain a large portion of cellular membrane, were labeled slowly and to substantially lower specific activity. Plasma membrane (PM) also labeled slowly, achieving a specific activity only one-sixth that of ER at 15 min in $HSDM_1C_1$ cells (6% of total label) and one-third of ER in EPU-1B (10% of total label). Nuclear membrane (NM) exhibited the highest specific activity of labeling at 15 min in $HSDM_1C_1$ cells (twice that of ER) but was not preferentially labeled in the mutant. Over 24 h, PM label intensity increased to that of ER in both cell lines. However, NM activity diminished in $HSDM_1C_1$ cells by 24 h to a small fraction of that in ER. In response to agonists, $HSDM_1C_1$ cells release labeled arachidonate for icosanoid synthesis most readily when they have been labeled for short times. Our results therefore suggest that NM and ER, sites of cyclooxygenase in murine fibroblasts, are probably sources for release of [^{3}H]arachidonate, whereas PM and mitochondria are unlikely to be major sources of icosanoid precursors.

Arachidonic acid ($C20:4_{\Delta5,8,11,14}$) is the major polyunsaturated fatty acid of most mammalian cells and occurs primarily esterified in the *sn*-2 position of cellular phospholipids (11). In addition to serving as a structural membrane component, arachidonate is the primary substrate for the synthesis of icosanoids. These oxygenated metabolites, including prostaglandins, leukotrienes, thromboxane, and related compounds, modulate important biological processes including inflammation, allergy, and hemostasis (30). Icosanoid precursor fatty acids (chiefly arachidonate) are used by specific metabolic pathways, distinct from those used by other fatty acids, in cells that make these mediators. These cell types avidly accumulate arachidonate from their surroundings and esterify it into cellular lipids by virtue of an acyl-CoA synthetase specific for icosanoid precursor fatty acids (20, 34). A mutant cell line that lacks this enzyme is defective both in high affinity arachidonate uptake and its subsequent release in response to the agonist bradykinin (19).

Upon appropriate stimulation, icosanoid synthesis is initiated by the selective release of arachidonate from phospholipids, chiefly phosphatidylinositol and phosphatidylcholine. In every case studied thus far, the availability of unesterified arachidonate, and hence this specific release process, is the rate-limiting step for icosanoid production (16). Even in cells such as human platelets, which exhibit highly active icosanoid production, no more than 10–20% of cellular arachidonate is

released in response to maximal stimulation (3). Most cell types and tissues release substantially less than 10%. The basis for this limitation is not known. The specificity of arachidonate release is explained in part by the fact that phosphatidylinositol is highly enriched with arachidonate (~80% of its molecules), but not all phosphatidylinositol is degraded upon stimulation, and some released arachidonate must be derived from phosphatidylcholine, which is not enriched with icosanoid-precursor fatty acids (3).

One possible explanation for the specificity and limited extent of arachidonate release is structural compartmentalization within cells. We undertook the present study in order to better define the pathways of arachidonate metabolism at a cellular level. Our goals were to evaluate the kinetics of distribution of arachidonate among subcellular compartments, to determine whether any particular structure became enriched in short- or long-term labeling, and to use these results to help elucidate the intracellular pathways for polyunsaturated fatty acid metabolism.

[^{3}H]Arachidonic acid is well suited to evaluation by electron microscope (EM)[1] autoradiography. Commercially available tritiated arachidonate contains nearly four ^{3}H atoms per molecule, so that high levels of cell radioactivity can be achieved using low (nanomolar) concentrations of label. Furthermore, the polyunsaturated acyl moiety of arachidonoyl phospholipids enhances cross-linking by osmium tetroxide, thereby providing spatial fixation of radiolabeled molecules during tissue processing for electron microscopy. We used $HSDM_1C_1$ murine fibrosarcoma cells, which, unlike many other permanent lines, release arachidonate and produce an icosanoid (Prostaglandin E_2) in response to stimuli such as bradykinin or ionophore A23187 (31). The $HSDM_1C_1$ cells exhibit high affinity arachidonate uptake and esterification, but also are viable in medium devoid of arachidonate and all essential fatty acids (15).

We also examined a mutant variant of $HSDM_1C_1$ cells, designated EPU, selected for defective high affinity uptake of arachidonate. Six independently selected clones of these cells (one of which is EPU-1B) lack the arachidonate specific acyl-CoA synthetase. Formation of acyl-CoA is the first step in incorporation of fatty acid into cellular lipids. Thus EPU-1B cells take up and esterify arachidonate at one-half to one-third the normal rate. Furthermore, EPU-1B cells are defective in arachidonate release, although their phospholipase C and A_2 activities are apparently normal (19). We analyzed uptake of [^{3}H]arachidonate in the mutants to determine whether the lack of arachidonoyl-CoA synthetase might affect the observed subcellular distribution of arachidonate, and whether differences in distribution might account for the defective EPU arachidonate release.

MATERIALS AND METHODS

Cell Culture: $HSDM_1C_1$ murine fibrosarcoma cells (American Type Culture Collection, Rockville, MD) and EPU-1B mutants (variants of $HSDM_1C_1$ with defective high affinity uptake of arachidonate) were grown in continuous culture as previously described (15, 19). Cells were plated 2 d before labeling in 35-mm polystyrene dishes (Corning Glass Works, Corning, NY) at densities of $0.5–1.0 \times 10^5$ per dish.

Labeling: [5,6,8,9,11,12,14,15-^{3}H]Arachidonic acid (88 Ci/mmol) was obtained from New England Nuclear (Boston, MA). Growth medium was removed from each dish and the cells were washed with 1 ml serum-free F10 medium (KC Biologicals, Kansas City, MO). 5 μCi of tritiated arachidonate was then added in 1.0 ml of F10 medium containing 4.2% delipidated horse serum (9). The final arachidonate concentration was 60 nM. At the end of the labeling time course, the medium was removed, each dish was washed twice with 0.5 mg/ml fatty acid–free albumin (Sigma Chemical Co., St. Louis, MO) in buffer (15.4 mM Tris-Cl, pH 7.4, 140 mM NaCl, 2.6 mM KCl, 5.6 mM glucose, 0.5 mM $MgCl_2$, 0.9 mM $CaCl_2$), and fixative was added.

Tissue Processing for EM: During processing, cells remain attached to the culture dishes. Cells were fixed in 2% glutaraldehyde plus 1.5% tannic acid, postfixed with 2% osmium tetroxide, stained en bloc with 0.5% uranyl magnesium acetate, dehydrated in ethanol, and infiltrated with Epon resin as previously described (13). In selected experiments, the amount of radioactivity removed from cells during each processing step and retained by cells at the completion of processing was assessed with liquid scintillation spectrometry as previously reported (13).

Preparation of Autoradiographs: Autoradiographs were prepared according to a modification of the flat-substrate method of Salpeter and Bachmann (28) as previously described (27). Polymerized Epon resin containing processed cells was separated from each polystyrene culture dish and cut into small fragments. For cross-sectioning, fragments were flat-embedded in Epon and the blocks sectioned in a plane perpendicular to the plane of the culture dish. For *en face* sectioning, fragments were glued to acrylic stubs and sectioned in a plane parallel to the plane of the culture dish. In each experimental condition, at least five randomly selected fragments of embedded cells were sectioned for autoradiographic analysis. Background control sections were prepared from unlabeled cultures of $HSDM_1C_1$ cells which were processed for electron microscopy and placed on the same slides as the radiolabeled tissue sections. Previous studies have demonstrated no significant artifacts due to positive or negative chemography or latent image fading in the autoradiography procedures used in these studies (26).

Exposure intervals ranged from 7 to 23 d. The emulsions were developed in 1.1% *p*-phenylenediamine and 12.6% sodium sulfite and fixed in 30% sodium thiosulfate. Sections were collected on 200 mesh copper grids and examined with a JEOL 100C electron microscope at 60 keV. Tissue processing with tannic acid and uranyl magnesium acetate provided adequate contrast so that further staining of the sections was unnecessary. Thus, possible removal of developed silver grains due to alkaline lead citrate stains (24) was avoided.

The physical developer *p*-phenylenediamine yielded developed grains which were compact rather than filamentous, thus minimizing obstruction of underlying fine structure of the specimen by the grains (4). This developer has a measured efficiency of approximately 1 grain per 15 disintegrations (1). The half-distance for the autoradiographic system used in these studies is ~1,500 Å, measured by Salpeter et al (29) using tritium, monolayers of Ilford L-4 emulsion, 100-nm thick sections, and *p*-phenylenediamine development.

Analysis of Autoradiographs: Autoradiographs were analyzed according to the mask overlay method of Salpeter et al. (29), using the computer program of Land and Salpeter (14), (generously supplied by Dr. M. Salpeter, Cornell University). A final print magnification of 40,000 was chosen for analysis. To avoid potential biases in selecting only certain regions of cells for analysis, composite photomicrographs were constructed to permit analysis of sections of entire cells or large portions of entire cells. For each condition analyzed, composites produced from at least 10 separate cells were analyzed. More than 4,000 individual electron micrographs were prepared. Most of the blocks were sectioned *en face*, roughly parallel to the original plane of the tissue culture dish, in order to maximize the sectional area of the cells. Mask data for all $HSDM_1C_1$ or EPU-1B cells sectioned in this plane were pooled for the source-grain matrix and area analyses. In conditions where cells were sectioned perpendicular to the dish, unique sets of mask data were used. A total of 297 to 1621 autoradiographic grains were tabulated for each condition in the arachidonate labeling experiments.

Potential sources, encompassing the entire photographic surface area, included membranous organelles, nonmembranous cellular structures (cytoplasm and nucleus), and extracellular areas of the photographs. Sources of radioactivity were expected to reside in cell membranes since most radioactivity was incorporated into phospholipids. Therefore, we analyzed mainly membrane sources including the plasma membrane (PM), endoplasmic reticulum (ER), nuclear membrane (NM), mitochondria, and other cytoplasmic membrane structures (CMS). The "CMS" compartment was a heterogeneous source including lysosome and phagosome membranes (but not their contents), coated vesicles (but not coated pits clearly attached to plasma membrane), and any other membranous structures that did not resemble other organelles. Because of the manner in which this compartment was defined, CMS could have included atypical portions of ER.

[1] *Abbreviations used in this paper:* EM, electron microscope; ER, endoplasmic reticulum; NM, nuclear membrane; PM, plasma membrane; CMS, other cytoplasmic membrane structures.

RESULTS

Incorporation and Preservation of [^{3}H]-Arachidonate in Cell Lipids

[^{3}H]Arachidonate was rapidly incorporated into lipids of $HSDM_1C_1$ and EPU-1B cells. More than 70% of the added label was removed from the labeling medium by cells at 2 h of incubation. The bulk of [^{3}H]arachidonate was incorporated into phospholipids. For example, in $HSDM_1C_1$ cells after 2 h of incubation, ~94% of radioactivity taken up was incorporated into phospholipids and 4% was found in neutral lipids as determined by thin layer chromatography (13). These results for arachidonate incorporation into $HSDM_1C_1$ and EPU-1B cells are consistent with those previously reported (15, 19, 31). Extraction of cell radioactivity during tissue processing was minimal. As shown in Table I, 92–96% of incorporated radioactivity was retained in cells during fixation and tissue processing. Nearly half of the radioactivity extracted during processing was neutral lipid; no single species of phospholipid was selectively extracted (13).

Analysis of Autoradiographs

Table II lists the source compartments and their relative areas as determined by mask analysis of the autoradiographs. More than 85% of the photographic surface area comprised the nonmembranous structures, cytoplasm, extracellular area, and nucleus. Golgi apparatus was encountered too infrequently to be adequately analyzed by the computer method.

TABLE I. *Preservation of [^{3}H]Arachidonic Acid in Cellular Lipids*

Cells	Labeling interval	Total radioactivity before processing	Percent of total cell radioactivity retained
		dpm/dish	
$HSDM_1C_1$	15 min	1.10×10^6	92.2
$HSDM_1C_1$	2 h	6.33×10^6*	93.4*
EPU-1B	2 h	2.29×10^6*	94.6*
$HSDM_1C_1$	24 h	5.12×10^6	96.4
EPU-1B	24 h	4.85×10^6	96.1

Duplicate dishes for each condition shown were analyzed for preservation of label during processing for autoradiography. Radioactivity extracted at each step in fixation and dehydration was measured and compared to the amount retained in tissue at the completion of processing (13).
* Determined in a separate experiment.

TABLE II. *Photographic Surface Area of Source Compartments*

Compartments	Percent total area	
	$HSDM_1C_1$	*EPU-1B*
Extracellular areas	12.5	11.3
Cytoplasm	54.9	41.9
PM	1.20	1.30
Mitochondria	4.90	4.50
Golgi apparatus	0.25	0.27
ER	4.00	3.11
NM	0.83	0.95
Nucleus	21.0	35.9
CMS	0.52	0.65

Source-grain pair mask data from *en face* sections of each cell type were pooled to give greater accuracy in surface area determination. Total photographic area analyzed for $HSDM_1C_1$ cells was ~10 m^2 of photos (16,100 source-grain pairs, 6,500 μm^2 cell area). For EPU-1B cells, 14 m^2 of photographs were analyzed (18,700 source-grain pairs, 8,700 μm^2 cell area). Grain compartments included the source compartments listed here, plus "rim" compartments, one half-distance wide, for PM, mitochondria, Golgi apparatus, ER, NM, and CMS.

The subcellular distribution of arachidonoyl phospholipids was determined by analyzing EM autoradiographs (see Fig. 1) of $HSDM_1C_1$ and EPU-1B cells labeled with arachidonate for 15 min, 40 min, 2 h, and 24 h as described in Materials and Methods. The computer-generated source distributions from this experiment, expressed as grains per μm^2 structure area, are shown in Table III for $HSDM_1C_1$ cells and in Table IV for the EPU-1B mutant. In the best-fit distribution of sources, cytoplasm, nucleus, and extracellular areas contained no radioactivity in either cell line. This result is a validation of the analysis method, since virtually all cellular phospholipid is expected to be in membranes, and >90% of [^{3}H]arachidonate was incorporated into phospholipids at all times in the labeling experiment. Unlabeled cells demonstrated negligible background grain density (~0.1 grains/100 μm^2) at the longest exposure time.

The amount of radioactivity per unit area of each structure represents a relative "specific activity," reflecting the avidity or rapidity with which a structure accumulated arachidonate. Thus, for example, at 15 min, NM and CMS were most intensely labeled in $HSDM_1C_1$ cells, ER was intermediate in specific activity, and PM and mitochondria were considerably less radioactive (Table III). To determine total radioactivity per compartment, we multiplied specific activity per unit area by the fractional area of each compartment. The result for each time point in the labeling time course of both cell lines is shown in Fig. 2. The combined information from Tables III and IV and Fig. 2 provides information about the uptake and distribution of the label among membrane compartments.

PM: PM was notable for its very low activity early in the labeling time course for both cell lines. Although the radioactive arachidonate in the medium must traverse the plasma membrane en route to internal structures, it apparently was not sequestered there. At 15 min after labeling, PM contained only 6% of incorporated arachidonate in the parental cells and 10% in the mutants (Fig. 2) and the intensity of labeling was a small fraction of that in ER (Tables III and IV). Thus, although EPU-1B cells exhibited overall lower levels of uptake, labeling intensity in PM was equivalent at the earliest time point. The apparent low label intensity at 40 min in Table IV was associated with a large standard error from the computer analysis, and thus may not represent a trough in PM labeling. By 24 h in both cell types, PM had attained a specific activity similar to that of ER, suggesting that these pools equilibrated by slow movement of arachidonate-containing lipids to PM from more highly labeled pools (ER and NM) after the bulk of label had been incorporated (i.e., after 2 h).

ER: ER contained more than half of the cell-associated [^{3}H]arachidonate at all times in the $HSDM_1C_1$ labeling time course, and exhibited the highest intensity of all compartments at 24 h (approximately steady state). Thus, ER is a major site for both incorporation and storage of arachidonate. Over the course of labeling in $HSDM_1C_1$ cells, it was relatively enriched at the expense of label intensity in NM and CMS. These pools did not appear to transfer label to ER in the EPU-1B cells, so that at 24 h, ER contained slightly less than half of incorporated arachidonate. However, ER labeling was qualitatively similar in control and mutant cells.

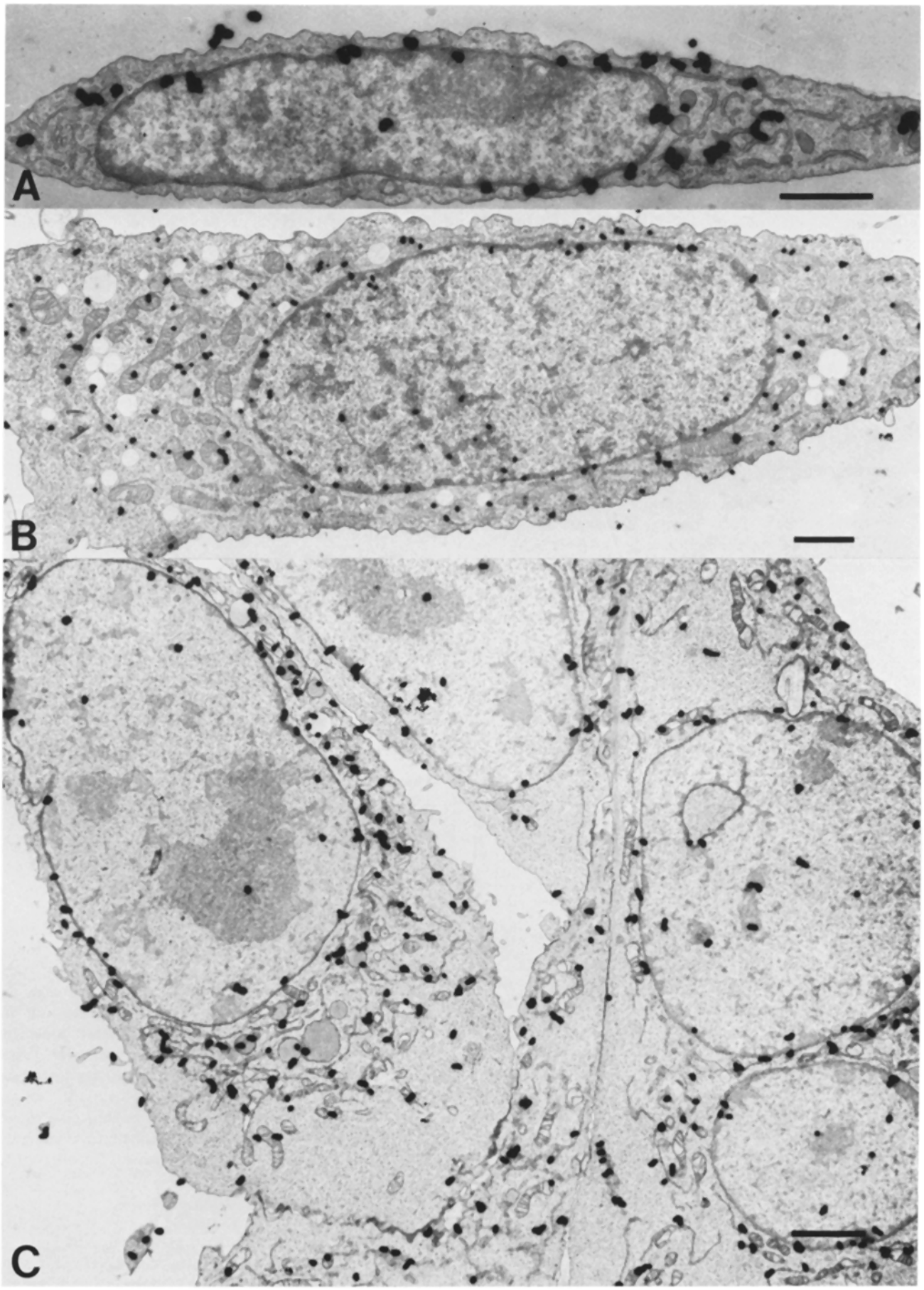

FIGURE 1 Representative autoradiographs of $HSDM_1C_1$ and EPU-1B cells. Cells were labeled with [^{3}H]arachidonate and processed as described in Materials and Methods. (*A*) $HSDM_1C_1$ cells cross-sectioned in a plane perpendicular to the tissue culture dish. (*B*) EPU-1B and (*C*) $HSDM_1C_1$ cells sectioned *en face* in a plane parallel to the culture dish. The intensity of labeling is low in the nucleus, structure-free peripheral cytoplasm, and extracellular areas. Bar, 1 μm. (*a*) × 8,400; (*b*) × 5,400; (*c*) × 6,500.

TABLE III. *Time Course of [^{3}H]Arachidonate Labeling Intensity In Source Compartments of HSDM$_1$C$_1$ Cells*

Compartments	Grain density (grains per μm^2)			
	15 min	*40 min*	*120 min*	*24 h*
Extracellular areas	0.0	0.0	0.0	0.0
Cytoplasm	0.016 ± 0.05*	0.0	0.0	0.0
PM	1.25 ± 0.9	1.74 ± 1.0	4.70 ± 3.0	40.4 ± 6.3
Mitochondria	0.69 ± 0.2	0.40 ± 0.2	4.80 ± 1.1	12.5 ± 1.3
ER	6.20 ± 0.6	13.0 ± 0.8	24.1 ± 2.7	50.0 ± 3.6
Nucleus	0.02 ± 0.03	0.0 ± 0.03	0.0 ± 0.09	0.0 ± 0.09
NM	11.7 ± 1.6	10.2 ± 1.7	19.3 ± 3.4	4.10 ± 3.0
CMS	13.9 ± 2.6	14.7 ± 3.1	4.7 ± 4.3	36.2 ± 10

Source intensity at each labeling time point, as calculated by the Chi-square minimization routine of Land and Salpeter (14), was converted to grains per μm^2 by correcting for the photographic surface area in each condition. The 120-min results are the means from two separate culture dishes. Data are normalized to an emulsion exposure time of 545 h.

* Error values shown represent the standard error of the Chi-square minimization routine (14).

TABLE IV. *Time Course of [^{3}H]Arachidonate Labeling Intensity In Source Compartments of EPU-1B Cells*

Compartments	Grain density (grains per μm^2)			
	15 min	*40 min*	*120 min*	*24 h*
Extracellular areas	0.0	0.0	0.0	0.0
Cytoplasm	0.0	0.0	0.0	0.0
PM	1.28 ± 0.3*	0.08 ± 0.9	9.90 ± 3.6	31.6 ± 3.4
Mitochondria	0.33 ± 0.09	0.40 ± 0.2	4.10 ± 1.1	15.6 ± 1.3
ER	3.40 ± 0.3	26.5 ± 2.7	27.1 ± 2.8	39.3 ± 2.1
Nucleus	0.0 ± 0.01	0.01 ± 0.03	0.0 ± 0.09	0.0 ± 0.08
NM	3.30 ± 0.8	4.70 ± 1.5	37.5 ± 6.5	31.1 ± 6.5
CMS	2.81 ± 0.5	0.64 ± 0.8	13.3 ± 3.8	50.5 ± 5.9

Source intensities for interval in the EPU-1B labeling experiment were calculated as described in the legend of Table III. The 120-min results represent the means of data from two separate dishes. The results are corrected to an emulsion exposure time of 545 h.

† Standard errors of the Chi-square minimization routine.

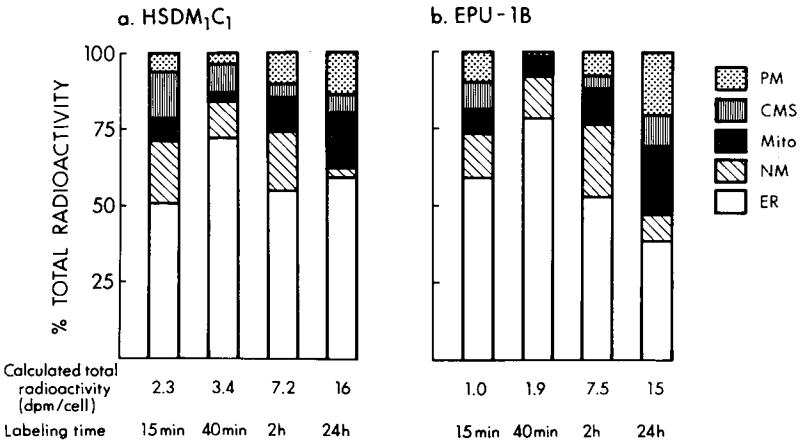

FIGURE 2 Time course of distribution of [^{3}H]arachidonate among cellular compartments. Cells were labeled for various times, and autoradiographs prepared and analyzed as described in Materials and Methods. The intensity of labeling in each compartment was multiplied by the fractional area of each compartment and is expressed as percentage of total cell-associated radioactivity at each time point. Total cellular radioactivity was calculated by adding activity in all compartments, and correcting for duration of exposure, estimated cell volume, and reported photographic efficiency. Totals for 2- and 24-h points are not directly comparable due to different numbers of cells in different conditions. (*a*) HSDM$_1$C$_1$ cells. (*b*) EPU-1B cells. *PM*, plasma membrane; *Mito*, mitochondria; *ER*, endoplasmic reticulum; *NM*, nuclear membrane; *CMS*, other cytoplasmic membrane structures.

NM: NM was labeled to a high specific activity at the earliest time point in HSDM$_1$C$_1$ cells, suggesting a kinetic advantage in arachidonate esterification. As label was consumed in the first two hours of incorporation, however, other pools caught up with and surpassed the NM labeling intensity; despite a kinetic preference for arachidonate, the level is relatively excluded from this pool at steady state. Although the 24-h NM value in Table III is associated with a large error because of the relatively small number of grains encountered, the qualitative conclusion would be unchanged even if actual NM labeling were at the upper limit of the error range. EPU-1B cells did not preferentially label NM. The pool was equal to ER in intensity at 15 min. NM also did not become relatively unlabeled at 24 h in the mutant as it did in HSDM$_1$C$_1$ cells.

MITOCHONDRIA: Mitochondria were labeled less intensely than other membranes at all times, but this deficit was more pronounced in short-term labeling (≤2 h), when this pool had specific activity <20% of that in ER. At 24 h, the mitochondria had not equilibrated with the other pools, and contained only a small fraction of total cellular label. (Some portion of the difference in specific activity may have been due to the manner in which mitochondrial surface area was calculated.[2])

CMS: In both cell lines, this small, heterogeneous pool

[2] The mitochondrial source compartment included both inner and outer membranes and their contents (unlike other membrane compartments, defined to exclude all nonmembrane surface), because it was not possible to distinguish folds of inner membrane sectioned in the plane of the membrane from membrane-free matrix and because of the many, closely spaced cristae. This inclusion of matrix may have exaggerated the area of the source somewhat, and therefore underestimated true specific activity in mitochondrial membranes, without affecting the calculation of total compartment radioactivity.

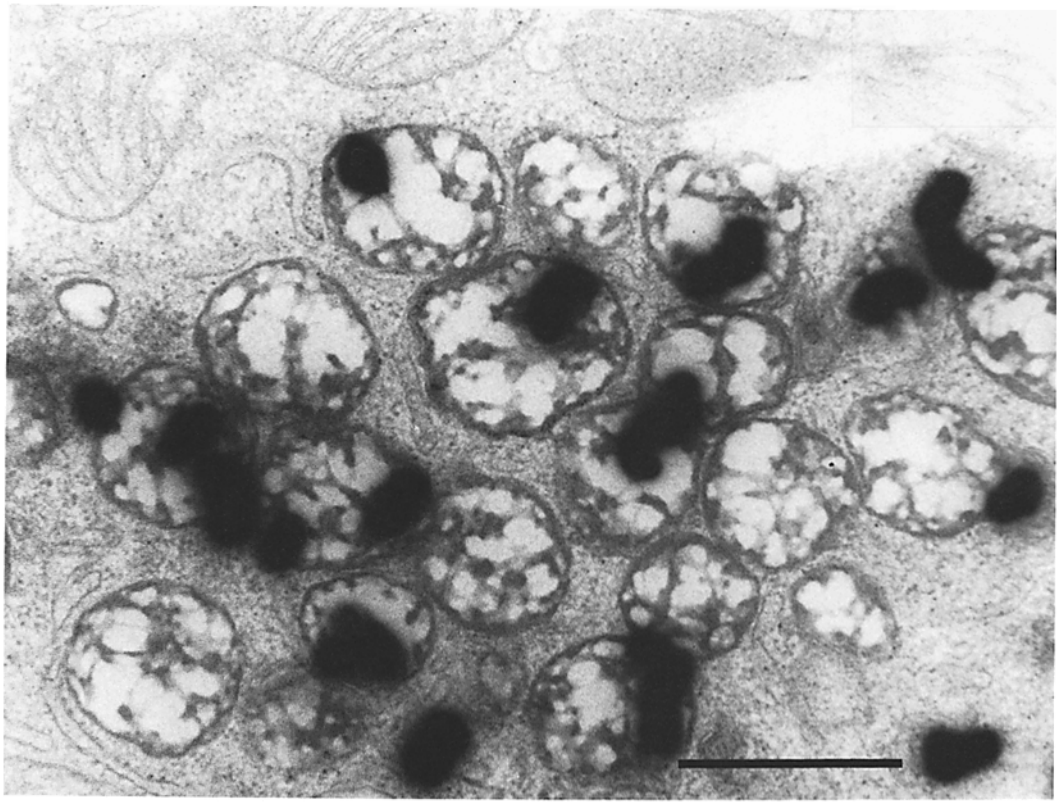

FIGURE 3 Phagosome-like bodies in EPU-1B cells labeled for 24 h with [^{3}H]arachidonate. Structures of this type were more common in EPU-1B cells than $HSDM_1C_1$. This autoradiograph shows a region where they were particularly numerous. The membranes of these structures were included in the heterogeneous CMS pool. Bar, 1 μm. × 29,000.

contained few grains at early time points, and thus exhibited relatively large standard errors (Tables III and IV). In $HSDM_1C_1$ cells, CMS was highly labeled at the 15-min time point, despite the fact that, because of its small area, it accounted for little of total cellular label. In EPU-1B cells, labeling intensity was highly variable: similar to ER at 15 min, very low at 40 min, and the most intensely labeled pool at 24 h (Table IV). At least part of the high intensity labeling in this pool at later time points was caused by the presence of [^{3}H]arachidonate in phagosome-like structures which were much more frequent in the mutant than in $HSDM_1C_1$ cells (Fig. 3).

GOLGI APPARATUS: Golgi apparatus was not encountered often enough to yield consistent results with the mask-overlay method. Our impression from the micrographs was that stacks of Golgi cisternae were not highly labeled at any time, but that peri-Golgi membranes (many of which were vesicular or lamellar structures designated "ER" on the basis of appearance) were more intensely labeled (Fig. 4).

Labeling Intensity of Coated Pits vs. PM

Large numbers of coated pits were observed in the plasma membranes of both $HSDM_1C_1$ and EPU-1B cells. In the analyses reported in Tables III and IV, coated pits clearly attached to the cell surface were included in the PM pool, whereas coated vesicles not attached to PM were assigned to CMS. We compared the labeling intensity of the pits to that of PM in the 24-h autoradiographs from both cell lines in order to determine whether these structures were in equilibrium with each other at steady state, or whether the pits, which turn over rapidly in the process of receptor-mediated endocytosis (22) had distinct arachidonate content. The labeling densities were estimated by the number of grains within one half-distance of the membrane per linear centimeter of PM or pit membrane. No significant difference in labeling intensity was detected (Table V). PM morphometry was not performed for autoradiographs at other time points. However, at 2 h after labeling, the fraction of total PM grains in or near coated pits was equivalent to that at 24 h. Thus, the rapid movement of membrane regions reflected by coated pits and vesicles does not result in differential rates of incorporation or turnover of icosanoid precursor fatty acids.

Calculation of Total Label Incorporation per Cell from Grain Densities

One method to determine whether the autoradiographic results obtained accurately reflect actual cellular labeling is to calculate total radioactivity per cell based on the observed grain density. Each pale gold microtome section was assumed to be 0.1 μm thick; the efficiency of the photographic process was estimated to be 1 grain per 15 disintegrations (1), and the exposure time 545 h. The volume of a typical cell was estimated to be ~900 μm^3 based on an average thickness determined from electron micrographs of sections cut perpendicular to the culture dish (Fig. 1) and cell surface area calculated from light photomicrographs of subconfluent cells in culture. (An equivalent size estimate was obtained by measuring the diameter of round, trypsinized cells by light microscopy.)

The estimates of total reactivity per cell are shown in Fig. 2 for $HSDM_1C_1$ and EPU-1B cells at each time point. Totals for the short-term and 24-h points are not directly comparable

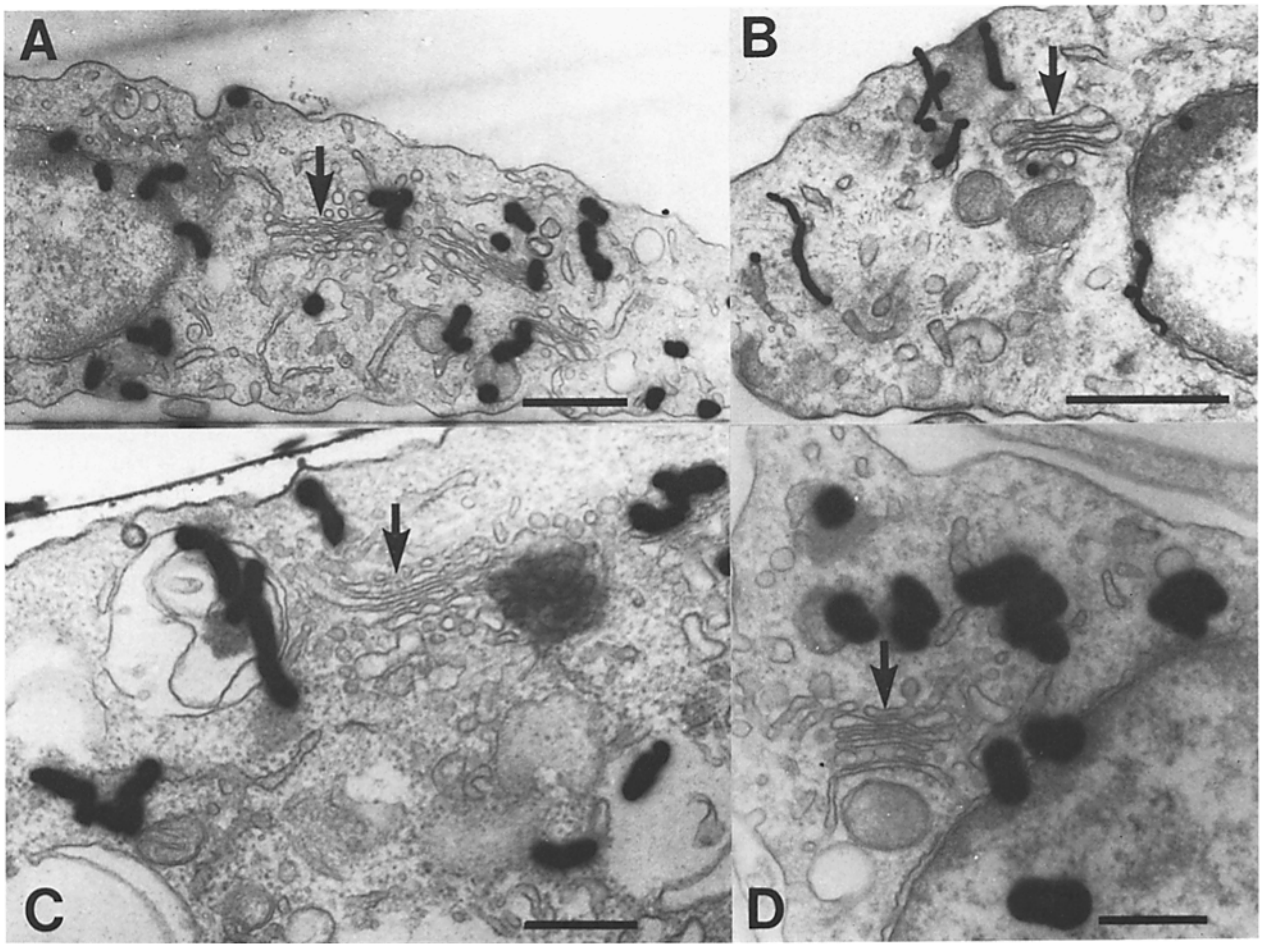

FIGURE 4 [^{3}H]Arachidonate labeling of peri-Golgi regions. Autoradiographs of $HSDM_1C_1$ cells labeled for 2 h. Grains are prevalent in regions surrounding stacks of Golgi cisternae (arrows), which are relatively less labeled. One-half distance = 0.15 μm. Bar, (*a* and *b*) 1 μm; (*c* and *d*) 0.5 μm. (*a*) × 14,000; (*b*) × 22,000; (*c*) × 29,000; (*d*) × 29,000.

TABLE V. *Label Intensity of Coated Pits vs. PM*

	PM length	Coated pits	PM grains	Pit grains	Grain density (grains/cm)	
	cm				*PM*	*pits*
$HSDM_1C_1$	1,600	66	116	6	0.075	0.091
EPU-1B	2,500	170	147	13	0.063	0.076

Total length in centimeters of PM in the photomicrographs from 24-h labeling of EPU-1B and $HSDM_1C_1$ cells was determined by computer-assisted planimetry. The length of an average coated pit was estimated by measuring the diameter of several from different cells. Grains within one half-distance of pits and PM were tallied and labeling intensity estimated as grains per unit length of membrane. Exposure time was 162 h.

because of differences in cell number per dish. The values (maximum labeling, ~16 dpm per cell) agree well with the estimate of uptake per cell obtained by counting the labeling medium before and after 24 h culture with the cells (25–40 dpm per cell).

DISCUSSION

Pathways of Arachidonate Incorporation

Details of the specific metabolic pathways and cellular compartments involved in formation of arachidonate-containing phospholipids have not been well defined. Fatty acids presumably gain access to internal compartments by diffusion through membranes because of their lipophilic nature. Hoak et al. (10) demonstrated by EM autoradiography that [^{3}H]-palmitate could readily diffuse into and out of platelet PM, depending on the presence of fat-free albumin, a fatty acid "trap" in the incubation medium. The cellular trap for arachidonate, and the enzyme responsible for high affinity cellular arachidonate uptake is the arachidonate-specific acyl-CoA synthetase (19, 20). The subcellular localization of this membrane-bound enzyme is unknown. The nonspecific long chain acyl-CoA synthetase has been located on the cytoplasmic face of rat liver microsomes (6).

Acyl-CoA esters are converted to phospholipids either by transfer of fatty acids to glycerol phosphate forming phosphatic acid (*de novo* synthesis) or by transfer to a pre-existing lysophospholipid ("Lands' pathway"). Arachidonate probably enters largely by the latter route (for review see reference 11). The site of arachidonate incorporation thus depends both on the distribution of synthetic enzymes and the availability of lysolipid precursors. The enzymes of *de novo* phospholipid synthesis are all found in "microsomes" of rat liver; some of the activities are also found in mitochondria. Lysophospholipid acyltransferases have been variously claimed to be localized to mitochondrial and microsomal fractions (reviewed by Bell and Coleman [2]).

Localization of Cellular Phospholipids

The subcellular distribution of newly synthesized lipids has been examined by EM autoradiography of [^{3}H]glycerol and

[^{3}H]choline incorporation in frog retina (17). Rough ER of rod inner segment was found to contain the bulk of incorporated label as well as the highest specific activity with short labeling pulses (10 min). NM was also relatively enriched with label, while smooth ER, Golgi apparatus, mitochondria, and PM were less intensely labeled. These results therefore demonstrate label distribution similar to our short-term arachidonate labeling. Nuclear membrane has also been implicated as an early source of lipid precursor incorporation in myeloma cells, in which pulses of radiolabeled acetate first label a rapidly sedimenting pool whose radioactivity is subsequently chased to other membrane fractions (23).

Measurement of endogenous fatty acid distribution has proven problematic because of difficulties obtaining purified membrane fractions with good yields and the tendency of lipids to migrate from membrane to membrane. Despite these difficulties, the phospholipid and fatty acid compositions of major membrane pools have been determined for rat liver cells. Colbeau et al. (5) found that PM was relatively deficient in arachidonate compared to ER and mitochondria. In another study, ER was found to be relatively enriched in arachidonate compared to PM and the Golgi apparatus (12). These results differ from ours in that we found PM equal in intensity to ER at steady state.

Struck and Pagano (32) and Sleight and Pagano (33) have demonstrated apparent organelle preference for certain types of lipids in live cells by tracing the transfer of lipid analogs from liposomes to Chinese hamster fibroblasts by fluorescence microscopy. They have found that fluorescent derivatives of phosphatidylethanolamine and phosphatidylcholine are initially restricted to PM (32) and subsequently move via endocytosis to Golgi apparatus (33). These studies probably measure bulk membrane flow, a different process from fatty acid incorporation described here. However, a derivative of phosphatidic acid caused fluorescence primarily in NM, ER, and mitochondria under conditions where bulk flow would not occur (21).

The distribution of [^{3}H]arachidonate in mast cells and macrophages has been evaluated with EM autoradiography by Dvorak et al. (8). These workers found that the majority of autoradiographic grains in cells labeled overnight occurred over cytoplasmic "lipid bodies." These structures were highly labeled not only with arachidonate, but also with [^{3}H]palmitate, methyl choline, and myoinositol (7). Because all lipid precursors preferentially accumulated in these structures, conclusions about the avidity of lipid bodies for arachidonate, and about their role in icosanoid metabolism, will depend on results of more detailed metabolic studies of these organelles.

Our laboratories have begun to examine the subcellular distribution of [^{3}H]arachidonate in human platelets. In the process of this work, we have noted that leukocytes in the platelet preparations rapidly and preferentially accumulate labeled arachidonate in their nuclear membrane (Saffitz, J. E., M. Laposata, and P. W. Majerus, unpublished results). Although we have not further quantified this observation, it lends support to the concept that NM is a kinetically preferred pool for arachidonate incorporation.

Comparison of Uptake and Distribution of Arachidonic Acid in EPU-1B and HSDM$_1$C$_1$ Cells

In the present studies we have examined the time course of uptake and subcellular distribution of arachidonic acid into the membranes of an icosanoid-producing fibrosarcoma cell line and a variant line defective in arachidonoyl-CoA synthetase. We found that ER is the major cellular repository of arachidonate at all times in the labeling period (from 15 min to 24 h), while mitochondria, which contain a large fraction of cellular membrane, are labeled to substantially lower activity. In both cell lines, PM is labeled to a much lower intensity than ER at early labeling times, eventually equilibrating with ER at 24 h. No preferential early labeling of CMS was observed in the mutant. One major difference between mutant and control cells was the overall lower level of labeling per cell at 15 and 40 min after labeling, before a large portion of the label had been removed from the medium (Fig. 2). This lower rate of uptake was manifest in all pools except PM, and was most notable in NM. At 15 min, the fraction of total label in NM of EPU-1B was less than that in HSDM$_1$C$_1$, and total uptake was 40% of control values (Fig. 2), so that the absolute difference in NM labeling intensity was a factor of 4 (Table III vs. IV). Differences in labeling between control and mutant in most pools were relatively small at later times and did not suggest large differences in arachidonate distribution among compartments between the two cell lines.

Two possible mechanisms could account for the early preferential labeling of NM and its subsequent loss of label. One possibility is that NM is a true precursor pool, responsible for synthesis of lipids which subsequently move to other compartments. Another possibility is that NM phospholipids are more rapidly "remodeled" than other membranes, so that the NM is labeled most rapidly because of the availability of lysolipid acceptors in this compartment, but label is lost due to the "editing" phospholipases once the cellular [^{3}H]arachidonoyl-CoA pool is depleted. Similar reasoning can be used for the CMS compartment, which was highly labeled at early time points but lost label relative to other pools over time. In general, the initially observed distribution of label favors kinetically preferred pools (either membranes that are actively synthesizing new lipid, or rapidly remodifying old phospholipids with *sn*-2 fatty acids), whereas the 24-h distribution represents the steady state of incorporation into various membranes, akin to the endogenous fatty acid distribution. A plausible explanation for the mutant's inability to label rapidly remodeling pools is that EPU-1B cells, by virtue of lacking arachidonoyl-CoA synthetase, are deficient in [^{3}H]arachidonoyl-CoA relative to unlabeled, endogenous pools of acyl-CoA's which compete for incorporation into lysolipid precursors. We cannot distinguish from these experiments whether the observed differences between EPU-1B and HSDM$_1$C$_1$ are due solely to absent arachidonoyl-CoA synthetase. Furthermore, we do not know if the observed fatty acid distribution is unique to arachidonate or typical of non-icosanoid precursors as well.

Nevertheless, the present data help to answer the question of which cellular compartments contribute arachidonate released for icosanoid synthesis upon cellular stimulation. Although HSDM$_1$C$_1$ cells release <5% of endogenous arachidonate for prostaglandin synthesis in response to an agonist such as bradykinin, they release a substantially larger fraction of labeled arachidonate when the label is added for short times. At short incubation times (15 min), as much as 15–20% of label can be released from HSDM$_1$C$_1$ cells depleted of essential fatty acids (15). In short incubations in the present experiments, label is found predominantly in the ER of HSDM$_1$C$_1$ cells, with high labeling intensity in NM and CMS.

The decrease in release efficiency over time suggests that these smaller pools might be responsible as they lose their specific activity relatively quickly. Of these two pools, NM seems a more likely source; it is difficult to imagine that lysosomes and coated vesicles should have the machinery of release. Interestingly, the cyclooxygenase of murine fibroblasts has been localized by EM immunohistochemistry to the ER and NM (25). It may be that EPU-1B cells, which lack early high intensity labeling of NM, are defective in arachidonate release because of their inability to label this pool, although a causal relationship between these facts remains to be established. The very low early labeling intensity and total label concentration in PM and mitochondria makes these compartments unlikely sources for release of radiolabeled arachidonate. If PM were the source, it would have to be entirely depleted of label during stimulation at early times, but contribute only a small fraction of its label at later times in labeling time courses. Because of these results, we speculate that the substrate for icosanoid synthesis is released at the site of synthesis. If receptor-mediated arachidonate release occurs from internal membranes, a second messenger (such as calcium mobilization) must be responsible for transmitting a signal for hydrolysis to the ER and NM from the receptor at the PM.

We are grateful to David B. Wilson and Thomas M. Connolly for helpful discussions and moral support during analysis of the autoradiographs, and to Betsy Kramer and Louise Schoelch for photographic assistance.

This research was supported by grants HL-14147, Specialized Center of Research in Thrombosis, and HL-16634 and HL-17646, Specialized Center of Research in Ischemic Heart Disease, from the National Heart, Lung, and Blood Institute; and by National Institutes of Health Research Service Award, GM-07200, Medical Scientist, from the National Institute of General Medical Sciences.

Received for publication 31 January 1985, and in revised form 19 April 1985.

REFERENCES

1. Bachmann, L., and M. M. Salpeter. 1967. Absolute sensitivity of electron microscope autoradiography. *J. Cell Biol.* 33:299–305.
2. Bell, R. M., and R. A. Coleman. 1980. Enzymes of glycerolipid synthesis. *Annu. Rev. Biochem.* 49:459–487.
3. Bills, T. K., J. B. Smith, and M. J. Silver. 1977. Selective release of arachidonic acid from the phospholipids of human platelets in response to thrombin. *J. Clin. Invest.* 60:1–6.
4. Caro, L. G., and R. P. Van Tubergen. 1962. High resolution autoradiography. I. Methods. *J. Cell Biol.* 15:173–188.
5. Colbeau, A., J. Nachbaur, and P. M. Vignais. 1971. Enzymic characterization and lipid composition of rat liver subcellular membranes. *Biochim. Biophys. Acta.* 249:462–492.
6. Coleman, R. A., and R. M. Bell. 1978. Evidence that biosynthesis of phosphatidylethanolamine, phosphatidylcholine and triacylglycerol occurs on the cytoplasmic surface of microsomal vesicles. *J. Cell Biol.* 76:245–253.
7. Dvorak, A. M., M. E. Hammond, E. S. Morgan, and H. F. Dvorak. 1980. Ultrastructural studies of macrophages: in vitro removal of cell coat with macrophage inhibition factor (MIF)-containing lymphocyte culture supernatants; chloroform extraction, phospholipase digestion and autoradiographic studies. *J. Reticuloendothel. Soc.* 27:119–142.
8. Dvorak, A. M., H. F. Dvorak, S. P. Peters, E. S. Shulman, D. W. MacGlashan, K. Pyne, V. S. Harvey, S. J. Galli, and L. M. Lichtenstein. 1983. Lipid bodies: cytoplasmic organelles important to arachidonate metabolism in macrophages and mast cells. *J. Immunol.* 131:2965–2976.
9. Esko, J. D., and K. Y. Matsuoka. 1983. Biosynthesis of phosphatidylcholine from serum phospholipids in Chinese hamster ovary cells deprived of choline. *J. Biol. Chem.* 258:3051–3057.
10. Hoak, J. C., A. A. Spector, G. L. Fry, and B. C. Barnes. 1972. Localization of free fatty acids taken up by human platelets. *Blood.* 40:16–22.
11. Holub, B. J., and A. Kuksis. 1978. Metabolism of molecular species of diacylglycerophospholipids. *Adv. Lipid Res.* 16:1–125.
12. Keenan, T. W., and D. J. Morre. 1970. Phospholipid class and fatty acid composition of Golgi apparatus isolated from rat liver and comparison with other cell fractions. *Biochemistry.* 9:19–25.
13. Krueger, C. M., E. J. Neufeld, and J. E. Saffitz. 1985. Preservation of arachidonoyl phospholipids during tissue processing for electron microscopic autoradiography. *J. Histochem. Cytochem.* In press.
14. Land, B., and E. E. Salpeter. 1978. Basis for computer program for mask analysis of EM autoradiographs. *J. Cell Biol.* 76:142–144.
15. Laposata, M., S. M. Prescott, T. E. Bross, and P. W. Majerus. 1982. Development and characterization of a tissue culture cell line with essential fatty acid deficiency. *Proc. Natl. Acad. Sci. USA.* 79:7654–7658.
16. Majerus, P. W., S. M. Prescott, S. L. Hofmann, E. J. Neufeld, and D. B. Wilson. 1983. Uptake and release of arachidonate by platelets. *Adv. Prostaglandin Thromboxane Leukotriene Res.* 11:45–52.
17. Mercurio, A. M., and E. Holtzmann. 1982. Ultrastructural localization of glycerolipid synthesis in rod cells of the isolated frog retina. *J. Neurocytol.* 11:295–322.
18. Neufeld, E. J., D. B. Wilson, H. Sprecher, and P. W. Majerus. 1983. High affinity esterification of eicosanoid precursor fatty acids by platelets. *J. Clin. Invest.* 72:214–220.
19. Neufeld, E. J., T. E. Bross, and P. W. Majerus. 1984. A mutant $HSDM_1C_1$ fibrosarcoma line selected for defective eicosanoid precursor uptake lacks arachidonate-specific acyl-CoA synthetase. *J. Biol. Chem.* 259:1986–1992.
20. Neufeld, E. J., H. Sprecher, R. W. Evans, and P. W. Majerus. 1984. Fatty acid structural requirements for activity of arachidonoyl-CoA synthetase. *J. Lipid Res.* 25:288–293.
21. Pagano, R. E., K. J. Longmuir, O. C. Martin, and D. K. Struck. 1981. Metabolism and intracellular localization of a fluorescently labeled intermediate in lipid biosynthesis within cultured fibroblasts. *J. Cell Biol.* 91:872–877.
22. Pearse, B. M. F., and M. S. Bretscher. 1981. Membrane recycling by coated vesicles. *Annu. Rev. Biochem.* 50:85–101.
23. Phillips, A. H., and F. D. Vasington. 1984. Evidence that newly synthesized membrane phospholipid initially appears at a distinct site in an actively secreting myeloma cell and then is rapidly translocated to other membranes. *Fed. Proc. Fed. Am. Soc. Exp. Biol.* 43:1714.
24. Rodgers, A. W. 1979. Techniques of autoradiography. Elsevier/North Holland, Amsterdam. 143.
25. Rollins, T. E., and W. L. Smith. 1980. Subcellular localization of prostaglandin-forming cyclooxygenase in Swiss mouse 3T3 fibroblasts by electron microscopic immunocytochemistry. *J. Biol. Chem.* 255:4872–4875.
26. Saffitz, J. E., R. W. Gross, J. R. Williamson, and B. E. Sobel. 1981. Autoradiography of phosphatidylcholine. *J. Histochem. Cytochem.* 29:371–378.
27. Saffitz, J. E., P. B. Corr, B. I. Lee, R. W. Gross, E. K. Williamson, and B. E. Sobel. 1984. Pathophysiologic concentrations of lysophosphoglycerides quantified by electron microscopic autoradiography. *Lab Invest.* 50:278–286.
28. Salpeter, M. M., and L. Bachmann. 1972. Autoradiography. *In* Principles and Techniques of Electron Microscopy—Biological Applications M. A. Hyatt, editor. Van Nostrand-Reinhold, New York. Vol. 2. 221–278.
29. Salpeter, M. M., F. A. McHenry, and E. E. Salpeter. 1978. Resolution in electron microscope autoradiography. IV. Application to analysis of autoradiographs. *J. Cell Biol.* 76:127–142.
30. Samuelsson, B. 1981. Prostaglandins, thromboxanes and leukotrienes: formation and biological roles. *Harvey Lect.* 75:1–40.
31. Schremmer, J. M., M. L. Blank, and R. L. Wykle. 1979. Bradykinin-stimulated release of [^{3}H]arachidonic acid from phospholipids of $HSDM_1C_1$ cells: comparison of diacyl phospholipids and plasmalogens as sources of prostaglandin precursors. *Prostaglandins.* 18:491–503.
32. Struck, D. K., and R. E. Pagano. 1980. Insertion of fluorescent phospholipids into the plasma membrane of a mammalian cell. *J. Biol. Chem.* 255:5404–5410.
33. Sleight, R. G., and R. E. Pagano. 1984. Transport of a fluorescent phosphatidylcholine analog from the plasma membrane to the Golgi apparatus. *J. Cell Biol.* 99:742–751.
34. Wilson, D. B., S. M. Prescott, and P. W. Majerus. 1982. Discovery of an arachidonoyl-Coenzyme A synthetase in human platelets. *J. Biol. Chem.* 257:3510–3515.